Journal of New Materials for Electrochemical Systems 20, 135-140 (2017)

Structural, Electrical and Electrochemical Properties of $Mg_{0.55}Si_{1.9}Al_{0.1}Fe_{0.1}(PO_4)_3$ Ceramic Electrolytes

N.A. Dzulkurnain[1], N.A. Mustaffa[2] and N.S. Mohamed[3,*]

[1]School of Chemistry & Food Technology, Faculty of Science & Technology, National University of Malaysia, 43600 Bangi, Selangor, Malaysia
[2] Faculty of Applied Sciences, Universiti Teknologi MARA, 40450 Shah Alam, Selangor, Malaysia
[3]Centre for Foundation Studies in Science, University of Malaya, 50603 Kuala Lumpur, Malaysia

Received: April 15, 2017, Accepted: July 04, 2017, Available online: August 03, 2017

Abstract: *This study was undertaken to investigate the structural, electrical and electrochemical properties of Fe^{3+} substituted $Mg_{0.55}Si_{1.9}Al_{0.1}(PO_4)_3$ compound synthesized by water-based sol–gel technique. X-ray diffraction showed that the compound crystallized in monoclinic crystalline phase with a space group of P1 $2_1/c1$. The sample sintered at 850 ˚C exhibited the highest conductivity of 1.42×10^{-6} S cm^{-1} at 373 K since it contained the highest number of mobile ions. It also exhibited the highest value of ion mobility, μ of 1.13×10^{-11} cm^2 V^{-1} s^{-1} at ambient temperature which was attributed to the optimum size of migration channel as indicated by its unit cell volume. Linear sweep voltammetry result showed that the $Mg_{0.55}Si_{1.9}Al_{0.1}Fe_{0.1}(PO_4)_3$ was electrochemically stable up to 3.0 V. Meanwhile, its ionic transference number of 0.99 suggested that the majority of the mobile charge carriers were mainly to ions, expected to be Mg^{2+} ions.*

Keywords:

1. INTRODUCTION

Increasing demands for high-energy-rechargeable batteries have developed battery technology. Many types of rechargeable batteries have been developed so far. Among them, the rechargeable lithium ion battery has been recognized as the most suitable battery for mobile information devices due to its high energy and power densities [1]. However, safety issues of lithium batteries such as overcharging, overheating or short circuit may results in fire or explosion. This may be due to liquid electrolytes used in commercial battery suffer several drawbacks compared to solid electrolytes. The drawbacks include limited temperature range of operation, device failure due to electrode corrosion by electrolyte solution, leakage and unsuitable shapes [2]. So as an alternative, a suitable and ideal solid electrolyte with high ionic conductivity at operating temperature, low electronic conductivity and also good electrochemical stability toward electrodes are required to overcome these disadvantages. Among solid electrolytes, NASICON (Sodium Superionic Conductor) type ion conductors can be a suitable candidate to be applied in commercial batteries.

NASICON (Sodium Superionic Conductor) solid electrolyte was first discovered by Hong and Goodenough et. al [3, 4] with the general formula of $Na_{1+x}Zr_2Si_xP_3O_{12}$. It has a three-dimensional rhombohedral space group $R\bar{3}c$ with the corners being made up of ZrO_6 octahedra and PO_4 tetrahedra [5, 6]. Two ZrO_6 octahedra are separated by three (Si,PO_4) tetrahedra that share corner oxygen atoms and two types of Na sites (Na1and Na2) [7]. The two sodium sites, Na1 and Na2, inside the channels, are connected through triangular bottlenecks of oxygen atoms. The bottleneck between both sites of the rhombohedral symmetry is formed by three oxygen atoms whose centers make up an isosceles triangle. High ionic conductivity, due to the movement of sodium ions depends on the activation energy required for the movement of the ions and size of the bottleneck, which is related to lattice parameters, whose value can be modified by changing compositions [8].

Since the first discovery of NASICON-structured materials, various investigations have focused on lithium analogous NASICON-structured with the general formula of $LiM_2P_3O_{12}$ with M = Ti [9, 10], Hf [11, 12], Zr [13], Ge [14], Sn [15-18], etc . However, recently, many researchers have diverted the attention towards greener and environmentally benign materials that are Mg based materials. The replacement of Li^+ ions with Mg^{2+} ions process has been reported to be successful since the ionic radius dif-

*To whom correspondence should be addressed: Email: nsabirin@um.edu.my
Phone:

ference between Li^+ (0.69 Å) and Mg^{2+} ion (0.65 Å) is below 15%, which does not exceed the solubility limit for atomic radii differences in solid solution. The studies on the development of magnesium battery electrolytes using NASICON-structured compounds are still limited in number. Nomura et al. have performed a systematic investigation on the framework structure, phase transition and electrical conductivity of magnesium zirconium phosphates, $MgZr_4(PO_4)_6$ [19]. Anuar et. al successfully synthesized $Mg_{0.5}Zr_2(PO_4)_3$ parent compound that crystallized in monoclinic phase [20]. Partial substitutions of Fe^{3+} at Zr^{4+} site in the compound of $Mg_{0.5+y}(Zr_{2-y}Fe_y)_2(PO_4)_3$ [21] and double substitutions producing $Mg_{0.9+0.5y}Zn_{0.4}Al_yZr_{1.6y}(PO_4)_3$ compounds have also been studied [22]. Halim et. al (2016) studied the effects of sintering temperature on the structural, electrical and electrochemical properties of novel $Mg_{0.5}Si_2(PO_4)_3$ ceramic electrolytes [23].

In this work, water based sol-gel method was used to synthesize a new $Mg_{0.5+x/2}Si_{2-x}Al_xFe_x(PO_4)_3$ compound. Then the structural, electrical and electrochemical properties of the ceramic electrolytes were studied using X-ray diffraction (XRD), Fourier transform infrared (FTIR), impedance spectroscopy (IS), transference number measurements and linear sweep voltammetry (LSV).

2. EXPERIMENTAL PROCEDURE

2.1. Synthesis of $Mg_{0.5+x/2}Si_{2-x}Al_xFe_x(PO_4)_3$

$Mg_{0.5+x/2}Si_{2-x}Al_xFe_x(PO_4)_3$ samples for the present work were prepared by sol gel method. The starting materials were magnesium acetate tethrahydrate ($C_4H_6MgO_4{\cdot}4H_2O$), silicon dioxide (SiO_2), aluminium acetate ($AlC_6H_9O_6$), ammonium phosphate monobasic (H_6NO_4P) and iron (III) chloride ($FeCl_3$) while citric acid ($C_6H_8O_7$) was used as the chelating agent. The molar ratio of Mg:Si:Al:Fe:P:O was calculated based on the stoichiometric formula of $Mg_{0.5+x/2}Si_{2-x}Al_xFe_x(PO_4)_3$ (x = 0.1). The value of x was fixed of 0.1 to study the effect of substituting Fe^{3+} on $Mg_{0.55}Si_{1.9}Al_{0.1}(PO_4)_3$ compound. The starting materials were first dissolved separately in distilled water by magnetic stirring at temperature of 30°C. Solutions of the starting materials were mixed together and stirred in a reflux system at 70 °C for 24 hours to form a homogenous solution. The solution was evaporated for at least 7 hours under magnetic stirring at 80 °C. The resulting wet gel was dried in a vacuum oven at 150 °C for 24 hours to remove water particle and organic resistance. The obtained powder was later subjected to heating process at 400 °C for 4 h in order to remove ammonium and acetate groups. The powder samples were then heated at sintering temperatures of 800 °C, 850 °C and 900 °C for about 4 h.

2.2. Characterization of the samples

The X-ray powder diffraction analysis was done on the samples using PANalytical-X'pert^3 X-ray diffractometer with Cu-Kα radiation of wavelength of 1.5406 Å in 2θ range from 10° to 40°. The samples were subjected to FTIR analysis in order to confirm the formation of the crystalline phases by using Perkin Elmer Frontier FTIR spectrometer. The FTIR analysis was performed in the spectral range from 550 to 1400 cm^{-1} at a resolution of 2 cm^{-1}. The FTIR data were recorded in the transmittance mode.

Impedance spectroscopy was carried out to determine the conductivity of the studied samples. The bulk conductivity (σ_b) was calculated using equation:

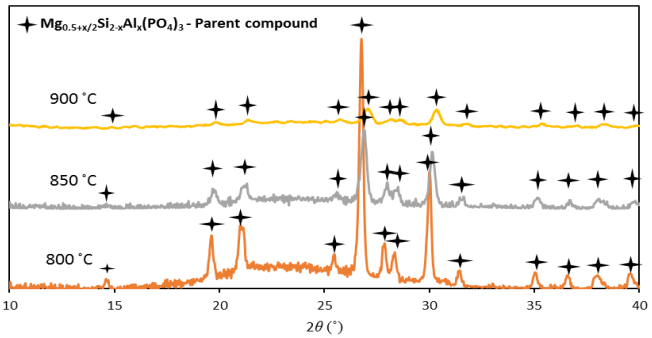

Figure 1. XRD spectra of $Mg_{0.55}Si_{1.9}Al_{0.1}Fe_{0.1}(PO_4)_3$ sintered at 800 °C, 850 °C and 900 °C.

$$\sigma_b = \frac{d}{AR_b} \quad (1)$$

where d is the sample thickness, A is the cross sectional area of sample and R_b is the bulk resistance obtained from the impedance spectra. The electrochemical stability window was obtained by LSV which was done using a Wonatech ZIVE MP2 multichannel electrochemical workstation.

AC conductivity, σ_{ac} values were calculated based on the relation:

$$\sigma_{ac} = \omega \epsilon_0 \epsilon'' \quad (2)$$

where ϵ_0 is the permittivity of the free space (8.854×10^{-14} F cm^{-1}) and ϵ'' is the dielectric loss [24, 25].

Wonatech ZIVE MP2 Multichannel electrochemical workstation was used to determine the total ionic transference numbers (τ_{ion}) of the sample based on the analysis of the dc polarization technique with stainless steel as the blocking electrodes. This is used to discriminate between electronic and ionic conduction in ceramic electrolytes. Meanwhile, the electrochemical stability window of the highest conducting sample was obtained using LSV. The LSV measurement was carried out in the range from -5 V to 5 V at a scanning rate of 100 m V s^{-1}, with stainless steel as the blocking electrodes at room temperature.

3. RESULT AND DISCUSSION

3.1. X-Ray Diffraction analysis

Depicted in Fig. 1 are the XRD spectra of $Mg_{0.55}Si_{1.9}Al_{0.1}Fe_{0.1}(PO_4)_3$ samples sintered at three different temperatures. The spectra of the samples sintered at temperatures of 800, 850 and 900 °C exhibit sharp and well defined peaks attributed to $Mg_{0.55}Si_{1.9}Al_{0.1}Fe_{0.1}(PO_4)_3$ compound. No other peaks of impurities are observed. This proves that pure $Mg_{0.55}Si_{1.9}Al_{0.1}Fe_{0.1}(PO_4)_3$ has been obtained and all the samples were generally well crystallized. However, the decreased of XRD peak intensity for sintering temperature of 850 and 900 °C was due to the volatilization of $Mg_{0.5+x/2}Si_{2-x}Al_xFe_x(PO_4)_3$ compound as indicated by TGA study. This was reported in our earlier article [23]. The pure $Mg_{0.55}Si_{1.9}Al_{0.1}Fe_{0.1}(PO_4)_3$ compound crystallized in monoclinic

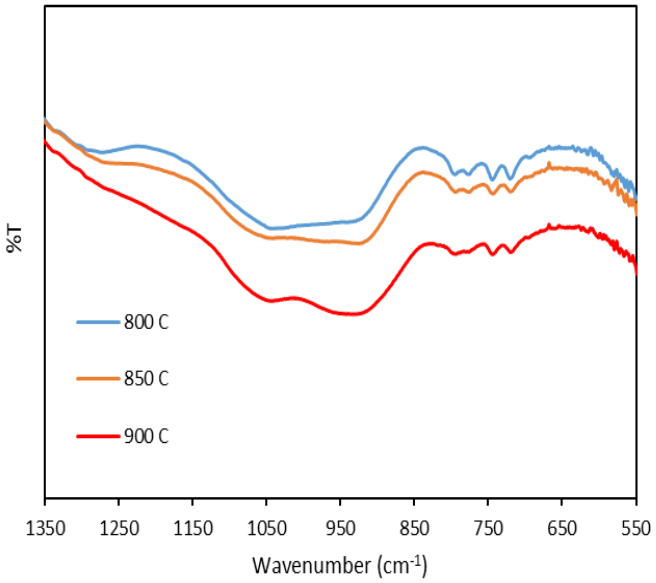

Figure 2. FTIR spectra of pure $Mg_{0.5+x/2}Si_{2-x}Al_xFe_x(PO_4)_3$ samples sintered at sintering temperatures of (a) 800 (b) 850 and (c) 900 ˚C in the spectral region from 550 cm^{-1} to 1350 cm^{-1}.

structure with a space group of P 1 2_1/c 1.

The lattice parameters, crystallite size, density and unit cell volume of the $Mg_{0.55}Si_{1.9}Al_{0.1}Fe_{0.1}(PO_4)_3$ samples are listed in Table 1. The values of *a, b*, *c* and *V* (unit cell volume) increase as the sintering temperature increases from 800 to 850 ˚C but decrease for the sample sintered at temperature 900 ˚C. Meanwhile, the crystallite size shows an opposite trend. The decrease in crystallite size is due to a decrease in defect concentration as a result of decreased proportion of surface atoms [26]. Amongst all the three sintered samples, the highest density goes to the sample sintered at temperature of 850 ^oC which is ascribed to the close packing of smallest crystallites in the sample [27].

3.2. FTIR analysis

Fig. 2 shows the FTIR spectra of the $Mg_{0.55}Si_{1.9}Al_{0.1}Fe_{0.1}(PO_4)_3$ samples in the 550 cm^{-1} to 1350 cm^{-1} spectral region. All spectra show the same stretching and vibrational modes. In this spectral range, the stretching or vibrational bands of silicon and phosphate elements are found to be active. For clarity purpose, we divided the spectral into two regions which are presented in Fig. 3. The absorption peaks in the 750 – 850 cm^{-1} range are assigned to the vibrational mode of symmetric stretching of Si–O–Si while stretching vibration of P-O-P is observed in the range of 700 – 750 cm^{-1} (Fig. 3(a)). On the other hand, the vibrational mode of asymmetric stretching of Si–O–Si is seen in the 900 – 1100 cm^{-1} spectral range (Fig. 3(b)) [28, 29]. It can be observed that the peaks become more intense with temperature. This is attributed to an increase of the coordination of Fe^{3+} cation with the oxygen hence resulting in weakening the Si-O-Si and P-O-P and change in the lattice parameters as mentioned earlier.

Table 1. Lattice parameters, unit cell volume and crystallite size of $Mg_{0.55}Si_{1.9}Al_{0.1}Fe_{0.1}(PO_4)_3$

Sintering temperature	*a* (Å)	*b* (Å)	*c* (Å)	*V* (Å^3)	Crystallite size (Å)
800 ˚C	6.997	9.106	11.911	758.89	114.8
850 ˚C	7.255	9.025	12.648	828.15	113.7
900 ˚C	7.233	8.948	12.555	812.51	114.9

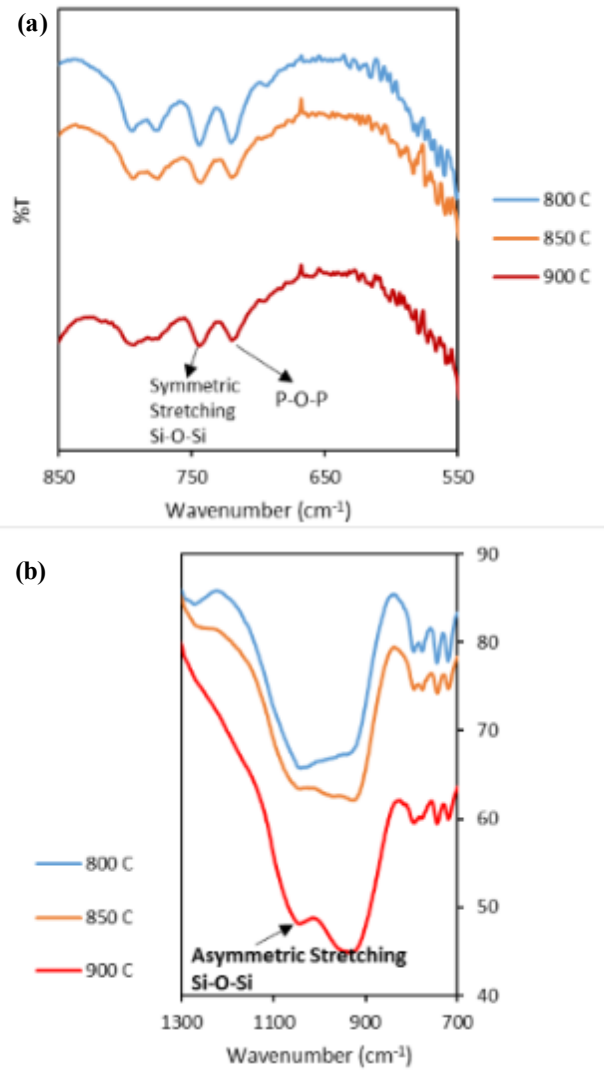

Figure 3. FTIR spectra of pure $Mg_{0.55}Si_{1.9}Al_{0.1}Fe_{0.1}(PO_4)_3$ samples sintered at sintering temperatures of 800, 850 and 900 ˚C in the spectral region (a) 550 to 850 cm^{-1} and (b) 700 to 1300 cm^{-1}.

3.3. Impedance analysis

The values of total conductivities for $Mg_{0.55}Si_{1.9}Al_{0.1}Fe_{0.1}(PO_4)_3$ compound measured at different temperatures are itemised in Table 2. For $Mg_{0.55}Si_{1.9}Al_{0.1}Fe_{0.1}(PO_4)_3$ compound sintered at 850 ˚C, the total bulk conductivity, σ_{bt} at 300 K is 9.09 × 10^{-8} S cm^{-1} which is a magnitude higher compared to those of the compounds that were sintered at 800 and 900 ˚C.

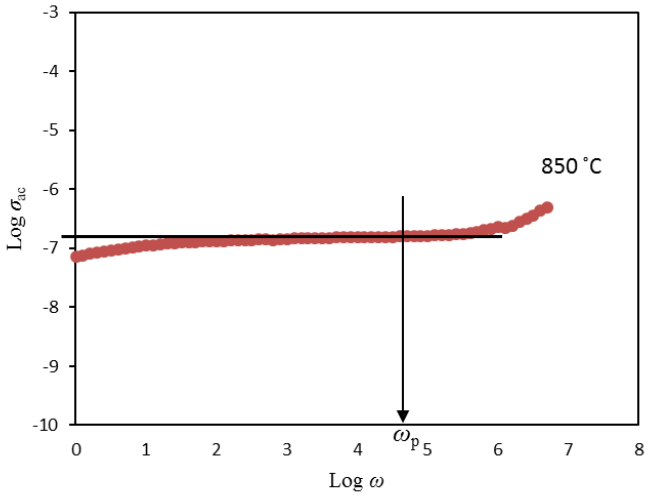

Figure 4. AC conductivity curve for $Mg_{0.55}Si_{1.9}Al_{0.1}Fe_{0.1}(PO_4)_3$ sample sintered 850 ˚C.

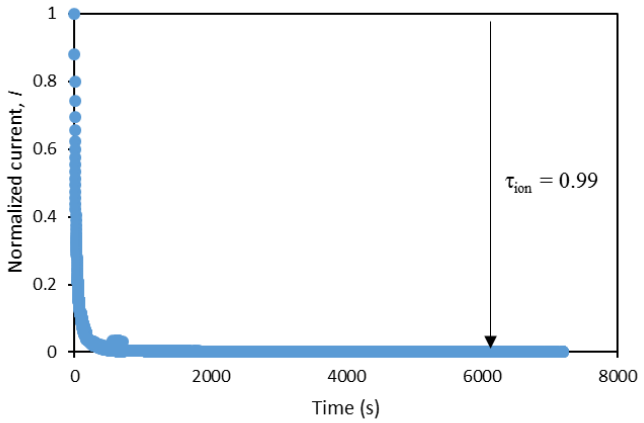

Figure 5. Plot of normalized polarization current versus time of $Mg_{0.55}Si_{1.9}Al_{0.1}Fe_{0.1}(PO_4)_3$ compound sintered at 850 ˚C.

According to Almond and co-researchers [30], the AC conductivity data can be utilized to estimate the ionic hopping rate, ω_p. ω_p can be determined by extrapolating at two times the value of DC conductivity from the vertical axis horizontally towards the graph and then extrapolating downwards vertically to the horizontal axis [24] as shown in Fig. 4. The plot shown in Fig. 4 contains a plateau in the intermediate frequency region and high frequency dispersion. The intermediate frequency plateau is due to the frequency independence of the conductivity corresponding to the DC conductivity.

Meanwhile, the magnitude of the charge carrier concentration, K, was calculated using the following equation [31-33] of:

$$K = \frac{\sigma T}{\omega_p} \tag{5}$$

where

$$K = ne^2a^2\gamma k^{-1} \tag{6}$$

In Eq. (6), e is the electron charge, γ is the correlation factor which is set equal to 1, and a is the jump distance between two adjacent sites for the ions to hope which is assumed to be 3 Å [24, 31, 33]. The density of the mobile ions (charge carrier), n, was calculated using Eq. 6, and k is the Boltzmann constant. The ionic mobility, μ, was determined using the expression as follows [27]:

$$\mu = \frac{\sigma_{dc}}{ne} \tag{7}$$

Table 3 lists the values of ω_p, K, n and μ at 100 ˚C for the $Mg_{0.55}Si_{1.9}Al_{0.1}Fe_{0.1}(PO_4)_3$ samples sintered at 800, 850 and 900 ˚C. The $Mg_{0.55}Si_{1.9}Al_{0.1}Fe_{0.1}(PO_4)_3$ compound sintered at 850 ˚C possessed the highest μ that is 1.13×10^{-11} cm^2 V^{-1} s^{-1}. This suggests that a decrease of the lattice size in the structure provided a more suitable tunnel size for the mobility of Mg^{2+} ions [34]. This sample also possessed the highest n. This gives another reason of why this sample exhibited the highest conductivity value.

3.4. Ionic transference number measurement

Fig. 5 displays a typical plot of normalized polarization current as opposed to time for $Mg_{0.55}Si_{1.9}Al_{0.1}Fe_{0.1}(PO_4)_3$ compound. The ionic transference number was evaluated from polarization current as opposed to time plot using the following classical equation:

$$\tau_{ion} = \frac{I_{initial} - I_{final}}{I_{initial}} \tag{8}$$

where $I_{initial}$ is the initial current and I_{final} is the final residual current (constant current). From the graph, it is illustrated that the total ionic transference number is 0.99 meaning that the conductivity of the $Mg_{0.55}Si_{1.9}Al_{0.1}Fe_{0.1}(PO_4)_3$ compound sintered 850 ˚C was predominantly due to the ions [35], which were expected to be Mg^{2+} ion.

Table 2. The σ_{bt} valuse of $Mg_{0.55}Si_{1.9}Al_{0.1}Fe_{0.1}(PO_4)_3$ samples sintered at 800 ˚C, 850 ˚C and 900 ˚C at three different temperatures.

Temperature of σ measurement	800 ˚C	850 ˚C	900 ˚C
27 ˚C	2.31×10^{-9} S cm^{-1}	9.09×10^{-8} S cm^{-1}	1.73×10^{-8} S cm^{-1}
80 ˚C	3.12×10^{-9} S cm^{-1}	1.55×10^{-7} S cm^{-1}	2.72×10^{-8} S cm^{-1}
100 ˚C	5.29×10^{-9} S cm^{-1}	1.42×10^{-6} S cm^{-1}	3.70×10^{-8} S cm^{-1}

Table 3. Value of ω_p, K, n and μ at 323 K for $Mg_{0.55}Si_{1.9}Al_{0.1}Fe_{0.1}(PO_4)_3$ samples sintered at 800, 850 and 900 ˚C.

Sintering temperature	ω_p (Hz)	K (S cm^{-1} K Hz^{-1})	n (cm^{-3})	μ (cm^2 V^{-1} s^{-1})
800 ˚C	2.01×10^3	5.02×10^{-10}	3.45×10^{22}	5.66×10^{-13}
850 ˚C	4.01×10^4	1.25×10^{-9}	8.59×10^{22}	1.13×10^{-11}
900 ˚C	3.19×10^4	2.76×10^{-10}	1.9×10^{22}	8.97×10^{-12}

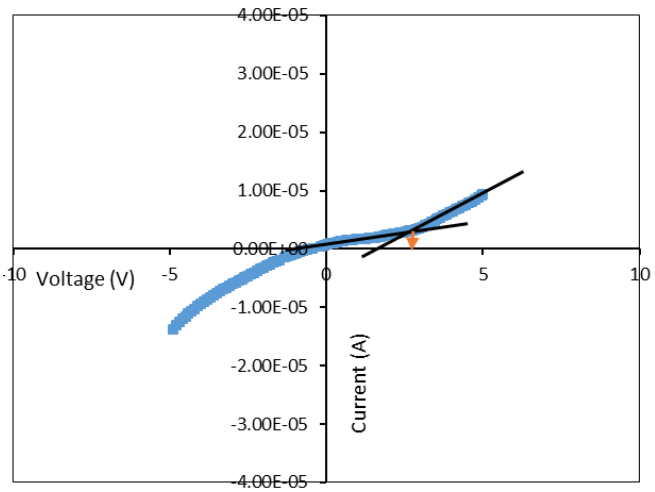

Figure 6. Linear sweep voltammogram of the $Mg_{0.55}Si_{1.9}Al_{0.1}Fe_{0.1}(PO_4)_3$ sintered at 850 ˚C with sweep rate of 50 mV s^{-1}.

3.5. Electrochemical stability window analysis

The electrochemical stability window was determined using linear sweep voltammetry in order to obtain the decomposition voltage of the $Mg_{0.55}Si_{1.9}Al_{0.1}Fe_{0.1}(PO_4)_3$ compound. Fig. 6 shows linear sweep voltammogram of the compound at room temperature. From the graph, the voltage stability window for the compound at room temperature was up to 3.0 V. The outcome displays that the $Mg_{0.55}Si_{1.9}Al_{0.1}Fe_{0.1}(PO_4)_3$ compound has potential to be used as an electrolyte in magnesium battery systems which require electrolytes that are electrochemically stable in the range of > 2.0 V [36].

4. CONCLUSIONS

Samples of $Mg_{0.55}Si_{1.9}Al_{0.1}Fe_{0.1}(PO_4)_3$ NASICON structured compound were successfully synthesized using sol-gel method with sintering temperatures of 800, 850 and 900 ˚C. The properties of the compound were influenced by the sintering temperatures. However, it was found that the sample sintered at 850 ˚C yielded the highest conductivity value. This was attributed to its optimum lattice size for ion migration as proven by the data of ion mobility values. Besides, this sample also contained the highest number of mobile ions. The $Mg_{0.55}Si_{1.9}Al_{0.1}Fe_{0.1}(PO_4)_3$ sample exhibited a wide and stable voltage window up to 3.0 V at ambient temperature. From the ionic transference number value (~ 1.0), it was inferred that the mobile charge carriers in this sample were mainly Mg^{2+} ions.

5. ACKNOWLEDGEMENT

The authors would like to extend their gratitude towards University of Malaya for allowing this research to be carried out. This work was supported by the University of Malaya Research Grant, RP013A-13AFR.

REFERENCES

[1] M. Kotobuki, M. Koishi, Ceramics International, 39, 4645 (2013).
[2] N. Anantharamulu, K.K. Rao, G. Rambabu, B.V. Kumar, V. Radha, M. Vithal, J. Mater. Sci., 46, 2821 (2011).
[3] H.Y.-P. Hong, Materials Research Bulletin, 11, 173 (1976).
[4] J.B. Goodenough, H.Y.-P. Hong, J.A. Kafalas, Materials Research Bulletin, 11, 203 (1976).
[5] J.W. Fergus, Solid State Ionics, 227, 102 (2012).
[6] P. Knauth, Solid State Ionics, 180, 911 (2009).
[7] W. Song, X. Ji, Z. Wu, Y. Zhu, Y. Yang, J. Chen, M. Jing, F. Li, C.E. Banks, Journal of Materials Chemistry A, 2, 5358 (2014).
[8] P. Yadav, M.C. Bhatnagar, Ceramics International, 38, 1731 (2012).
[9] H. Aono, E. Sugimoto, Y. Sadaoka, N. Imanaka, G. Adachi, Solid State Ionics, 40, 38 (1990).
[10]E. Zhao, F. Ma, Y. Jin, K. Kanamura, Journal of Alloys and Compounds, 680, 646 (2016).
[11]J. Kuwano, N. Sato, M. Kato, K. Takano, Solid State Ionics, 70, 332 (1994).
[12]C.-M. Chang, S.-H. Hong, H.-M. Park, Solid State Ionics, 176, 2583 (2005).
[13]K. Arbi, M. Ayadi-Trabelsi, J. Sanz, Journal of Materials Chemistry, 12, 2985 (2002).
[14]M. Illbeigi, A. Fazlali, M. Kazazi, A.H. Mohammadi, Solid State Ionics, 289, 180 (2016).
[15]R. Norhaniza, R.H.Y. Subban, N.S. Mohamed, Advanced Materials Research, 129-131, 338 (2010).
[16]N.A. Mustaffa, S.B.R.S. Adnan, M. Sulaiman, N. Mohamed, Ionics, 21, 955 (2015).
[17]N.A. Mustaffa, N.S. Mohamed, Int. J. Electrochem. Sci., 10, 5382 (2015).
[18]S. Tamura, M. Yamane, Y. Hoshino, N. Imanaka, Journal of Solid State Chemistry, 235, 7 (2016).
[19]K. Nomura, S. Ikeda, K. Ito, H. Einaga, Journal of Electroanalytical Chemistry, 326, 351 (1992).
[20]N.K. Anuar, S.B.R.S. Adnan, N.S. Mohamed, Ceramics International, 40, 13719 (2014).
[21]N.K. Anuar, S.B.R.S. Adnan, M.H. Jaafar, N.S. Mohamed, Ionics, 22, 1125 (2016).
[22]N.K. Anuar, N.S. Mohamed, Journal of Sol-Gel Science and Technology, 80, 249 (2016).
[23]Z.A. Halim, S.B.R.S. Adnan, N.S. Mohamed, Ceramics International, 42, 4452 (2016).
[24]S.B.R.S. Adnan, N.S. Mohamed, International Journal of Electrochemical Science, 7, 9844 (2012).
[25]N.A. Mustaffa, N.S. Mohamed, Journal of Sol-Gel Science and Technology, 77, 585 (2016).
[26]A. Gaber, M. Abdel-Rahim, A. Abdel-Latief, M.N. Abdel-Salam, J. Electrochemistry Sci., 9, 81 (2014).
[27]N.A. Mustaffa, S.B.R.S. Adnan, M. Sulaiman, N. Mohamed, Ionics, 1, (2014).

[28]F. Krok, Solid State Ionics, 24, 21 (1987).
[29]A. Gaber, M.A. Abdel-Rahim, A.Y. Abdel-Latief, M.N. Abdel-Salam, J. Electrochemistry Sci., 9, 81 (2014).
[30]D.P. Almond, G.K. Duncan, A.R. West, Solid State Ionics, 8, 159 (1983).
[31]L.P. Teo, M.H. Buraidah, A.F.M. Nor, S.R. Majid, Ionics, 18, 655 (2012).
[32]T. Savitha, S. Selvasekarapandian, C.S. Ramya, M.S. Bhuvaneswari, G. Hirankumar, R. Baskaran, P.C. Angelo, Journal of Power Sources, 157, 533 (2006).
[33]M. Vijayakumar, G. Hirankumar, M.S. Bhuvaneswari, S. Selvasekarapandian, Journal of Power Sources, 117, 143 (2003).
[34]E. Traversa, H. Aono, Y. Sadaoka, L. Montanaro, Sensors and Actuators B: Chemical, 65, 204 (2000).
[35]P.B. Bhargav, V.M. Mohan, A. Sharma, V.V.R.N. Rao, International Journal of Polymeric Materials, 56, 579 (2007).
[36]P. Saha, M.K. Datta, O.I. Velikokhatnyi, A. Manivannan, D. Alman, P.N. Kumta, Progress in Materials Science, 66, 1 (2014).